ELSEVIER

Journal of Nuclear Materials 279 (2000) 216–224

journal of nuclear materials

www.elsevier.nl/locate/jnucmat

Recovery characteristics of neutron-irradiated V–Ti alloys

T. Leguey, R. Pareja *

Departamento de Física, Universidad Carlos III de Madrid, Avda. de la Universidad 30, 28911 Leganés, Spain

Received 30 July 1999; accepted 14 January 2000

Abstract

The recovery characteristics of neutron-irradiated pure V and V–Ti alloys with 1.0 and 4.5 at.% Ti have been investigated by positron annihilation spectroscopy. Microvoid formation during irradiation at 320 K is produced in pure V and V–1Ti but not in V–4.5Ti. The results are consistent with a model of swelling inhibition induced by vacancy trapping by solute Ti during irradiation. The temperature dependencies of the parameter S in the range 8–300 K indicate a large dislocation bias for vacancies and solute Ti. This dislocation bias prevents the microvoid nucleation in V–4.5Ti, and the microvoid growth in V–1Ti, when vacancies become mobile during post-irradiation annealing treatments. A characteristic increase of the positron lifetime is found during recovery induced by isochronal annealing. It is attributed to a vacancy accumulation into the lattice of Ti oxides precipitated during cooling down, or at their matrix/precipitate interfaces. These precipitates could be produced by the decomposition of metastable phases of Ti oxides formed during post-irradiation annealing above 1000 K.

PACS: 61.80.Hg; 28.41.Qb; 61.82.Bg 78.70.Bj

1. Introduction

V alloys are low induced activation materials that have a high resistance to irradiation damage, excellent mechanical properties at high operation temperature and very low ductile–brittle transition temperatures (DBTT) [1–3]. In particular, V–Ti alloys with a Ti content around 5 wt% keep good mechanical properties and show no swelling after neutron irradiation up to very high fluences at temperatures in the range 470–870 K [2–11]. It is well established that the addition of some oversized solutes, such as Ti, Nb and Mo, promotes the swelling inhibition in V alloys [2,4,8,9,12]. The following models have been proposed to account for the swelling inhibition by Ti solutes. (1) The presence of an oversized solute such as Ti enhances the recombination between vacancies and self-interstitial atoms (SIA) [1]. (2) Ti atoms acting as interstitial impurity scavengers remove nucleation sites for microvoids [1]. (3) Ti-rich fine particles precipitated during irradiation act as very efficient vacancy sinks inhibiting the nucleation and growth of microvoids [7,11,13]. (4) Ti atoms are very efficient traps for radiation-induced vacancies; the high binding energy of the vacancy–Ti pairs hinders the vacancy migration preventing the microvoid nucleation at temperatures below 475 K [3,9]. In order to design optimized V–Ti alloys for nuclear applications, it is decisive, to elucidate which of the above-mentioned mechanism causes the swelling inhibition in these materials.

Positron annihilation spectroscopy (PAS) is an atom probe technique very sensitive to open-volume atomic defects giving valuable information about the microstructural interactions and stability of the irradiation-induced defects in metals. Thus, PAS appears to be a very useful method for investigating the mechanisms inhibiting the swelling in nuclear materials. The effect of Ti addition on the recovery of electron-irradiated and cold-rolled V–Ti alloys has been investigated by PAS [14,15]. The recovery of the mean positron lifetime $\langle\tau\rangle$ in electron-irradiated V–Ti alloys, with a Ti content $\leqslant 5$ at.%, starts at 460 K with the release of vacancies trapped by Ti atoms in solution. At annealing temperatures $T \geqslant 583$ K, these vacancies coalesce into microvoids which anneal out at temperatures above 780 K

* Corresponding author. Fax: +34-91 624 9430.
E-mail address: rpp@fis.uc3m.es (R. Pareja).

0022-3115/00/$ - see front matter
PII: S0022-3115(00)00013-1

[14]. 50% cold-rolled V–Ti alloys show recovery characteristics qualitatively different from those observed for electron-irradiated samples from the same batches [15]. The recovery is accomplished in two stages. Cold rolling induces microvoids in pure V, V–0.3Ti and V–1Ti but not in V–4.5Ti. In pure V, V–0.3Ti and V–1Ti, the recovery starts at about 500 K with the dissolution of these microvoids. The recovery curves of the annihilation parameters suggest the precipitation of fine Ti-rich particles induced by climbing dislocations during the first recovery stage. The second recovery stage, starting at about 1150 K, is attributed to annealing of vacancies associated to precipitates.

The above results indicate that: (1) dislocations and precipitates are decisive factors in the control of the growth and stability of the microvoids; and (2) Ti solutes delay the vacancy migration but they do not prevent the microvoid formation by themselves, at least for Ti content below 4.5 at.%. These conclusions point out that a PAS investigation of the recovery characteristics of V–Ti alloys neutron irradiated below the temperature for vacancy migration will contribute to a better knowledge of the swelling inhibition in these materials.

The present paper is organized as follows. In Section 2, the experimental procedure and some basic principles of the positron annihilation technique are described. The results for pure V, V–1Ti and V–4.5Ti are presented in Sections 3.1–3.3, respectively. The results for pure V are discussed in Section 4.1. The discussion of the characteristics of the first recovery stage for the alloys is given in Section 4.2 along with the mechanism inhibiting the microvoid formation. Section 4.3 deals with the second recovery stage of the alloys and gives an interpretation of the observed behavior of the annihilation parameters preceding this recovery stage.

2. Experimental method

2.1. Procedure

The materials used were 99.99% pure monocrystalline V and V–Ti alloys with Ti concentration of 1.0 and 4.5 at.%. Monocrystalline V samples were obtained from an electron beam zone-refined single crystal. The alloys were prepared from 99.9% pure V and 99.5% pure Ti by repeated arc melting in a high-purity argon atmosphere. The composition and homogeneity of the alloys were checked by X-ray fluorescence. Samples of the alloys, cut in slices about 1 mm thick, were successively cold rolled, polished and solution annealed to produce a free-defect reference state. The solution anneal was performed at 1573 K for 6 h in an oil-free vacuum of $<10^{-3}$ Pa. The pure V samples underwent the same heat treatment. After solution annealing the mean content of C, O and N in the V–Ti samples were 340, 290 and 20 wt ppm, respectively. The samples, inside an Al capsule filled with graphite, were exposed to a fast neutron flux of 0.78×10^{18} n/m^2 s up to a fluence of 1.04×10^{22} n/m^2 ($E>1$ MeV). The temperature of the capsule during the irradiation was 320 K.

Positron annihilation measurements in the temperature range 8–300 K were performed on the samples in as-irradiated state. Afterwards, positron lifetime measurements at RT were done after isochronal annealing for 30 min in steps of 30 K. The anneals above 400 K were made in an oil-free vacuum of $<10^{-3}$ Pa, below 400 K in a silicon oil bath. The positron annihilation experiments were made using a ^{22}Na positron source inserted between two identical samples. The source was enclosed inside sealed Kapton thin foils. A spectrometer with a time resolution of 230 ps (FWHM) was used. Doppler broadening measurements of the annihilation peak at 511 keV were made between 8–300 K after some annealing steps. These measurements were carried out with the samples inside a closed-He-cycle cryostat. A zero-and gain-stabilized high-purity Ge detector with an energy resolution of 1.62 keV at the 1.33 MeV was used.

Because of a failure in the temperature control program, the pure V samples were overheated while running positron lifetime measurements versus temperature. The temperature of these samples rose up to 350 K for 12 h, i.e. the collecting time of a lifetime spectrum; next it rose again reaching 533 ± 20 K for 4 h. Afterwards, the samples underwent the conventional isochronal annealing program.

2.2. Positron annihilation technique

A high-energy positron entering in a solid rapidly loses its energy until it reaches thermal equilibrium with the solid. After this thermalization process, the positron moves through the solid as a *free* particle characterized by a Bloch wave function (delocalized state). Vacancy-type defects, i.e., vacancies, vacancy–impurity pairs, dislocations, microvoids, ... etc, act as attractive centers to trap free positrons. Thus, a positron in a solid can annihilate with an electron either in the delocalized state or in a localized (trapped) state at a vacancy-type defect. The transition from the delocalized state to a trapped state is named positron trapping. The lifetime for a positron trapped, τ_t, depends on the local electron density and is longer than that for a delocalized positron in the bulk, τ_b. As a result of the presence of open-volume defects, the mean positron lifetime observed in a solid is expected to increase with radiation damage.

The positron lifetime spectrum from a solid is the sum of exponential terms. Each term corresponds to a different annihilation mode of the positrons in the solid. Thus, the number of terms, or components, in the spectrum should indicate, in principle, the number of

states in which the positrons annihilate in the solid. If only one type of defect acts as positron trap, the experimental lifetime spectrum can be fitted to a sum of two exponentially decay components given by the function [16]

$$P(t) = -N_0\left(\frac{I_1}{\tau_1}e^{-t/\tau_1} + \frac{I_2}{\tau_2}e^{-t/\tau_2}\right), \quad (1)$$

convoluted with the time resolution function of the spectrometer. N_0 is the total number of counts in the spectrum, $1/\tau_1 = \lambda_1$ and $1/\tau_2 = \lambda_2$ are the decay rates, and I_1 and I_2 are the relative intensities of the corresponding component. According to the standard two-state trapping model [16,17], λ_1, λ_2, I_1 and I_2 are related to the bulk lifetime, $\tau_b = 1/\lambda_b$, and the lifetime for trapped positrons, τ_t, by the equations

$$\tau_1^{-1} = \tau_b^{-1} + \kappa, \quad (2)$$

$$\tau_2 = \tau_t, \quad (3)$$

$$I_2 = 1 - I_1 = \frac{\kappa}{\kappa + \lambda_b - \lambda_2}, \quad (4)$$

where $\kappa = \mu C_t$ is the positron trapping rate, or transition rate from the delocalized state to the trapped one; κ is proportional to the defect concentration C_t and μ is the specific trapping rate for the defects. Two-component spectra are characterized by the mean positron lifetime given by

$$\langle\tau\rangle = I_1\tau_1 + I_2\tau_2. \quad (5)$$

When an experimental spectrum is *single-component,* it is accepted that (1) almost all positrons annihilate in the same state, delocalized or trapped depending on the defect concentration, or (2) if they do in more than one state, their decay rates are so close to each other that the different components cannot be separated. Moreover, lifetime spectra from samples containing different types of positron traps, i.e. more than one trapped state, can result in two-component lifetime spectra. For example, a sample containing microvoids and dislocations, or dislocation loops, should produce a three-component spectrum. However, the fitted spectrum very likely will be *two-component* because the positron lifetime for dislocations is close to the bulk positron lifetime. Then, the first spectral component would be a merged component from positrons annihilated in the bulk and in states localized at dislocations, while the second lifetime component τ_2 is the characteristic positron lifetime for microvoids. In order to reveal the presence of more than one type of positron traps in samples giving a two-component spectrum, the bulk lifetime calculated from Eqs. (2)–(4), i.e.

$$\tau_b = (I_1/\tau_1 + I_2/\tau_2)^{-1} \quad (6)$$

is compared to the experimental bulk lifetime measured in free-defect samples. A calculated value for τ_b significantly longer than the experimental one indicates that positrons annihilated in some trapped state contribute to the first component in addition to free positrons.

Thus, it is evident that the values of the annihilation parameters obtained from the lifetime spectrum, and their variations, can be used to identify the nature of the vacancy-type defects and their changes in a sample.

Also, the changes in the width of the annihilation peak at 511 keV give us information about the positron trapping in defects. The width is determined by the momentum of the annihilated positron–electron pairs since the energies of the annihilation photons are Doppler shifted. Annihilation with high-momentum electrons are more probable for delocalized positrons than for trapped positrons. This means, the narrower the annihilation peak the higher the positron trapping in defects. The Doppler broadening of the annihilation peak is usually characterized by the lineshape parameter called S [17].

In the present work, the lifetime spectra were analyzed using the programs RESOLUTION and POSITRONFIT [18]. The background and the source contribution to the spectra were subtracted after being determined from measurements on reference samples. The annihilation parameter S characterizing the Doppler broadening is the fraction of counts within an energy window of 1.50 keV centered at 511 keV.

3. Results

3.1. Pure V

As-irradiated samples show a two-component lifetime spectrum. Fig. 1 depicts the mean positron lifetime $\langle\tau\rangle$, the short lifetime τ_1 and the calculated bulk lifetime τ_b versus temperature, in the temperature range 10–350 K. The second lifetime component τ_2 remains essentially constant at 270 ± 30 ps over this temperature range but its spectral intensity I_2 increases continuously from 10.8% at 10 K to 44.1% at 297 K. After annealing at 533 K for 4 h, the lifetime spectrum continues being two-component but the $\langle\tau\rangle$ value at RT decreases from 208 to 140 ps, and the strong temperature dependence of the annihilation parameters becomes negligible as the Doppler broadening measurements shown in Fig. 2.

Isochronal anneals at $533 < T \leqslant 623$ K do not change the positron annihilation parameters significantly, τ_2 and I_2 remaining constant at 220 ± 15 ps and $16.5 \pm 2.5\%$, respectively. Fig. 3 shows the mean positron lifetime recovery as a function of the annealing temperature. For annealing temperatures above 623 K the positron lifetime starts to decrease continuously down to the bulk lifetime measured in the reference

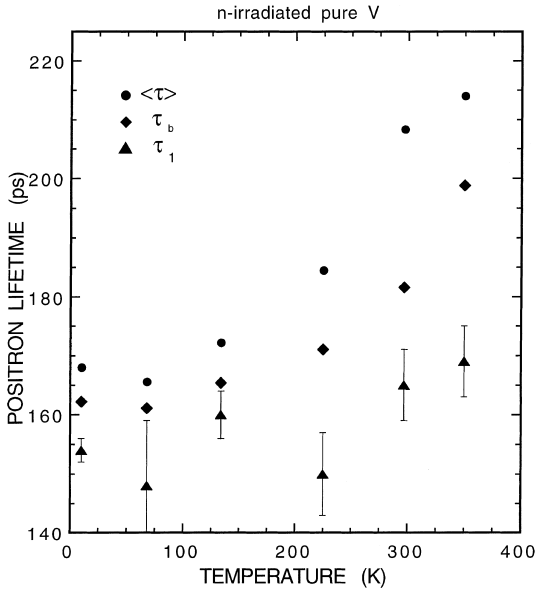

Fig. 1. Positron annihilation parameters $\langle\tau\rangle$, τ_1 and τ_b as a function of temperature for pure V neutron irradiated at 320 K. The second lifetime component stays constant at 270 ± 30 increasing its intensity I_2 from 10.8% at 10 K to 44.1% at 297 K.

samples, i.e. 124 ± 2 ps. The lifetime spectrum cannot be decomposed in two components after annealing at 683 K.

3.2. V–1Ti

The isochronal annealing effect on the annihilation parameters is shown in Figs. 3–5. The positron lifetime spectrum is two-component except after annealing in the interval $713 \leqslant T \leqslant 863$ K. Fig. 3 shows the recovery curve of the mean positron lifetime $\langle\tau\rangle$ along with those for pure V and V–4.5Ti; in the interval $713 \leqslant T \leqslant 863$ K the single lifetime of the observed spectrum is represented. The recovery is accomplished in two stages. The first starting at ~593 K ends at ~983 K. For annealing

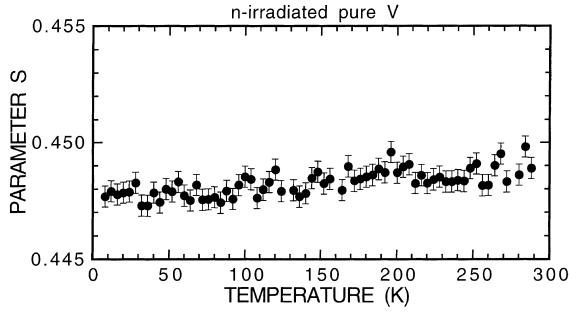

Fig. 2. Lineshape parameter S as a function of temperature for pure V post-irradiation annealed at 533 K.

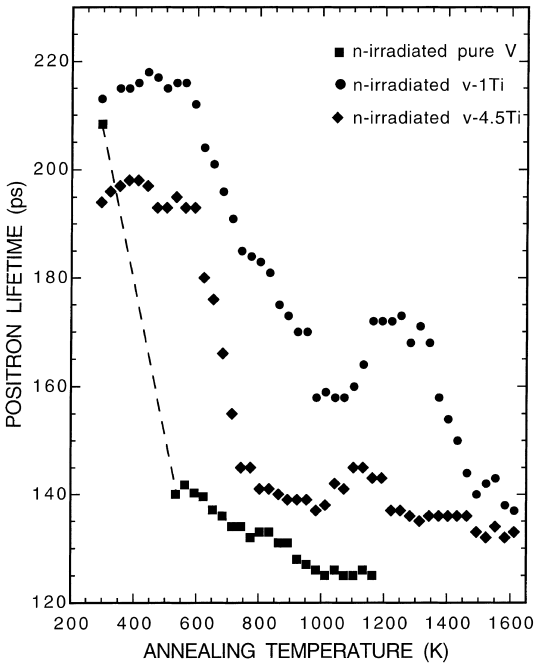

Fig. 3. Positron lifetime versus annealing temperature for pure V, V–1Ti and V–4.5Ti neutron irradiated at 320 K. The represented data show the mean positron lifetime $\langle\tau\rangle$ for pure V and V–1Ti, and the observed single lifetime for V–4.5Ti. The dashed line for the pure V data is drawn to guide the eye between the as-irradiated point and with those obtained after isochronal annealing experiments.

temperatures $T \geqslant 1103$ K, $\langle\tau\rangle$ increases from 158 ps to reach a constant value of 172 ps in the interval $1163 \leqslant T \leqslant 1313$ K. The second recovery stage starts above 1313 K. After annealing at 1613 K the lifetime spectrum is still two-component with a mean lifetime of 137 ps indicating that the complete recovery is not obtained yet.

Fig. 4 shows the variation of τ_2 and I_2 with the annealing temperature. The lifetime spectrum after annealing at $T \leqslant 713$ K reveals the presence of positron traps having a lifetime of 350 ± 30 ps. This is a characteristic lifetime for microvoids in metals. Its intensity I_2 stays at $14 \pm 3\%$ for annealing temperatures $T \leqslant 683$ K, indicating that the microvoid concentration does not change. They become unstable at annealing temperatures $T \geqslant 713$ K as the lifetime spectrum cannot be fitted to a sum of two exponential terms. After annealing at 863 K the lifetime spectrum is properly decomposed in two exponential terms again, revealing the appearance of new positron traps characterized by a lifetime of 194 ± 7 ps. The concentration of these defects appears to be constant in the interval $833 \leqslant T \leqslant 1103$ K. The increase of the $\langle\tau\rangle$ value observed after annealing above 1103 K is related to a change in the lifetime of the

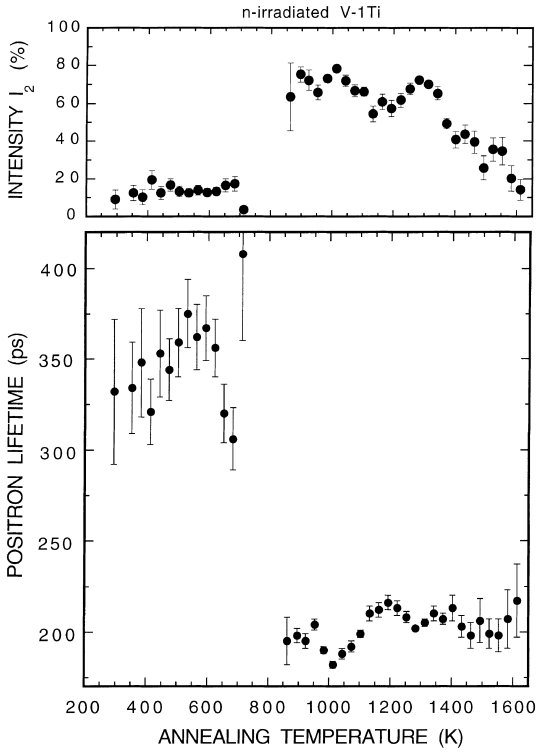

Fig. 4. Intensity I_2 and lifetime τ_2 of the second spectral component versus annealing temperature for V–1Ti neutron irradiated at 320 K. In the interval 713–863 K the lifetime spectrum is not decomposed into two components.

positron traps, as Fig. 4 shows. For annealing temperatures $1103 < T \leqslant 1613$ K, the τ_2 value remains constant at 207 ± 6 ps. The second recovery stage for $T \geqslant 1313$ K is mostly due to annealing of 207 ps traps as the variation of I_2 indicates.

Fig. 5 shows the lineshape parameter S as a function of temperature for the samples in as-irradiated state and after post-irradiation annealing. The temperature dependence is very strong for the as-irradiated samples. Post-irradiation annealing at $T \geqslant 533$ K reduces this temperature dependence noticeably.

3.3. V–4.5Ti

The samples in as-irradiated state and after post-irradiation annealing exhibit a single-component lifetime spectrum. Fig. 3 shows its positron lifetime as a function of the annealing temperature. As it occurs for V–1Ti, the positron lifetime recovery appears to be also accomplished in two stages. The onset and end of the first recovery stage coincides with the one for V–1Ti, approximately. The second recovery stage starts at about 1193 K. It is also preceded by a significant increase of the positron lifetime, although less prominent than the

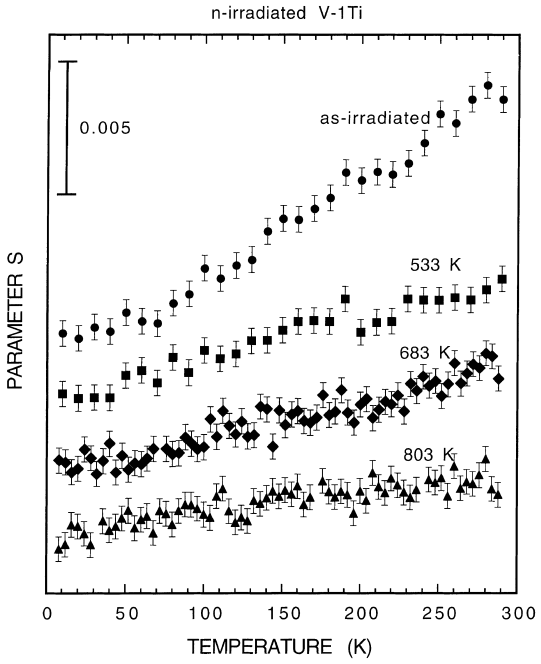

Fig. 5. Lineshape parameter S as a function of temperature for V–1Ti neutron irradiated at 320 K, and post-irradiation annealed at different temperatures.

one for V–1Ti. After annealing at 1613 K positron lifetime is 133 ps remaining far from the bulk lifetime for the V–4.5Ti alloy, i.e. 126 ps.

The results of the Doppler broadening measurements are shown in Fig. 6. The temperature dependence of the parameter S for the samples in as-irradiated state is significantly less strong than the one observed in the case of V–1Ti. An important qualitative difference with the results for V–1Ti is found. A negative temperature dependence appears after annealing at 683 K. The meaning of this qualitative change in temperature dependence of S will be discussed in Section 4.

4. Discussion

4.1. Pure V

The results indicate that the recovery of the these samples starts at annealing temperatures in the interval $350 < T < 533$ K. Because of the failure of the annealing program during measurements, the recovery onset has not been established accurately. In electron-irradiated V single crystals the recovery starts at about 400 K [14]. The second lifetime component of 270 ± 30 ps in the as-irradiated state indicates that single vacancies produced by neutron irradiation at 320 K perform long-range migration coalescing into small three-dimensional

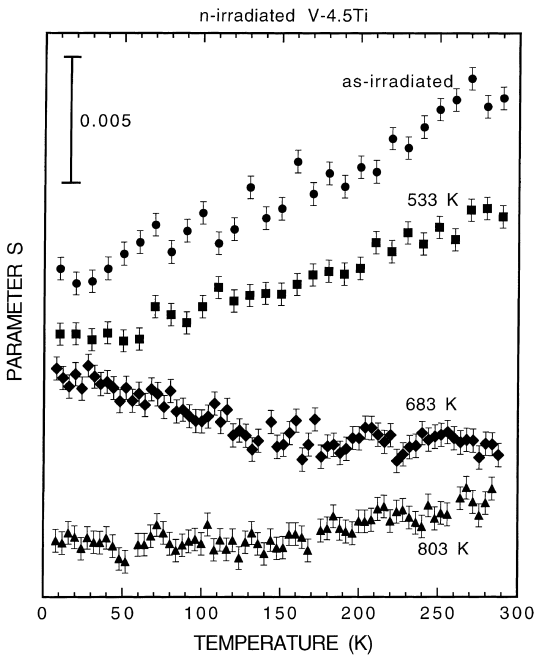

Fig. 6. Lineshape parameter S as a function of temperature for V–4.5Ti neutron irradiated at 320 K, and post-irradiation annealed at different temperatures.

vacancy clusters (microvoids). According to calculations, the expected radius for microvoids having a positron lifetime of about 270 ps would be between 0.2 and 0.3 nm [19]. This value is clearly smaller than the positron thermal wavelength; $\lambda\!\!\!^{-} = \hbar(2mk_{\mathrm{B}}T)^{-1} > 1.2$ nm for $T \leqslant 300$ K. This means that the positron specific trapping rate into these microvoids, μ, is temperature independent [20–22]. Therefore, the strong increase of $\langle\tau\rangle$ with increasing temperature shown in Fig. 1 cannot be attributed to a temperature dependence in the specific trapping rate for microvoids. The bulk lifetime values calculated by Eq. (6) do not agree with the experimental τ_{b} value of 124 ps indicating the presence of other positron traps in addition to microvoids. These traps contribute to the short lifetime component which is characterized by the lifetime value τ_1. The temperature dependences of annihilation parameters shown in Fig. 1 are explained if thermally activated positron detrapping from shallow traps is assumed. These shallow traps would be dislocations, vacancy-type dislocation loops or other microstructural defects with a relatively small positron binding energy and annihilation characteristics, lifetime and lineshape parameter S, experimentally indistinguishable from those for the bulk [23,24]. Shallow traps would act as effective traps at low temperatures competing for the positron trapping with deep traps such as vacancies, vacancy–impurity pairs and microvoids.

This is supported by the fact that annihilation parameters $\langle\tau\rangle$ and S are temperature independent after annealing at 533 K (see Fig. 2), in spite of the lifetime spectrum of the samples still exhibiting an intense long component due to microvoids. This shows that (1) the specific positron trapping rate into the microvoids is actually temperature independent, and (2) shallow and deep traps contributing to the short lifetime component start to anneal out at temperatures below 533 K. In these samples, microvoids become unstable at temperatures around 600 K as it occurs in the case of microvoids induced by cold rolling in samples from the same material [24].

4.2. V–Ti alloys. First recovery stage and inhibition of the microvoid formation

For V–1Ti and V–4.5Ti, the temperature dependence of S after annealing at 533 K differs from that observed for the samples in as-irradiated state, see Figs. 5 and 6. However, the annihilation parameters obtained from their respective lifetime spectrum measured at RT do not reveal significant changes until annealing above 600 K, as Figs. 3 and 4 show. According to the above-discussed arguments, this indicates that annealings at $T \leqslant 600$ K reduce the concentration of microstructural defects acting as shallow positron traps. In as-irradiated state the presence of shallow traps reduces the probability of trapping in microvoids and other deep traps at low temperatures, inducing a gradual decrease of the annihilation parameters $\langle\tau\rangle$ and S with decreasing temperatures. Then, the $S(T)$ curves exhibit a strong positive temperature dependence. The comparison of the $S(T)$ curves for V–1Ti and V–4.5Ti annealed at 533 K with those corresponding to pure V indicates that some shallow traps still survive after annealing at 533 K in the alloys but not in pure V. Thus, Ti solutes stabilize the microstuctural defects which act as shallow traps. Some of these defects can be present in V–1Ti after annealing at 803 K as the $S(T)$ curve suggests.

The negative dependence of $S(T)$ found for V–4.5Ti post-irradiation annealed at 683 K is consistent with a low-temperature enhancement of the positron trapping at deep traps via pre-trapping at shallow traps. We have previously investigated the annihilation characteristics in cold-rolled V demonstrating that the temperature dependence of the annihilation parameters $\langle\tau\rangle$ and S is the result of a temperature-dependent competing positron trapping in shallow and deep traps [24]. The model predicts a negative temperature dependence for $S(T)$ when the direct positron trapping rate at deep traps, κ_{13}, is smaller than the positron transition rate from dislocations to deep traps, κ_{23}. These deep traps in our neutron-irradiated V–Ti samples can be isolated vacancies or vacancy–solute complexes, and vacancy-type defects associated with dislocations, characterized by a positron

lifetime shorter than the one for microvoids. Also, vacancy–Ti complexes associated to vacancy-type dislocation loops are a scheme consistent with the above model of trapping at deep defects via pre-trapping at shallow traps. If these dislocation loops are formed in the V–Ti samples, it is reasonable to assume that they should be decorated with vacancy–Ti pairs. These Ti-decorated loops would be stable up to temperatures in the range $683 < T < 803$ K. However, the presence of microvoids in samples containing dislocation loops induces a positive temperature dependence for $S(T)$. It should be noted that a negative temperature dependence for $S(T)$ is not observed after annealing at 683 K when the microvoids have disappeared in pure V but they are still stable in V–1Ti. This indicates that either vacancy-type loops are not formed in pure V or Ti atoms stabilize them up to temperatures in the range 683–803 K.

After annealing at 683 K, the first lifetime τ_1 for V–1Ti is longer than the observed single lifetime for V–4.5Ti, i.e. 173 ps against 165 ps. This shows that the concentration of deep traps contributing to the first lifetime component in V–1Ti is higher than the defect concentration in V–4.5Ti annealed at the same temperature. Moreover, after annealing at 683 K the deep traps in V–4.5Ti have to be mostly associated with dislocations in order that the positron trapping rate at deep traps via pre-trapping at dislocations, κ_{23}, may be higher than the direct trapping rate κ_{13}. Previous results in electron-irradiated and cold rolled V–Ti alloys have shown that Ti solute is a very effective trap for vacancies, vacancy–Ti pairs and vacancy–Ti–interstitial impurity complexes being the defects responsible for the positron trapping [14,15]. Thus, in V–4.5Ti the deep positron traps associated with dislocations, and perhaps with dislocation loops, are very likely vacancy–Ti complexes. This means a large dislocation bias for solute Ti and vacancies. These complex defects decorating dislocations and dislocation loops can induce a high-energy barrier for SIA migration toward dislocations. This enhances the mutual recombination of vacancies and SIAs during irradiation and annealing, preventing the formation of microvoids in the V–4.5Ti alloy.

Another explanation for the inhibition of the microvoid formation can be given in terms of the effect of the solute Ti on the vacancy and interstitial production efficiency during irradiation. High concentrations of vacancies and SIAs are produced during the collisional phase. According to simulation experiments, vacancies and SIAs are heterogeneously distributed and spatially separated during this phase. Mutual recombination and clustering of vacancies and SIAs take place during the subsequent phase of the cascade, i.e. during the thermal-spike phase. Depending on the irradiation temperature, thermal-activated processes induce the evolution of the defect microstructure, so that an asymmetry in the production rate of free vacancies and SIAs can appear according to the stability of the respective clusters. Because of the elastic interaction between a vacancy and the oversized Ti solute, the mobility of vacancies is lower in V–Ti than in pure V. This can produce, in addition to a smaller fraction of agglomerated vacancies in the cascade region, remarkable differences between the vacancy and interstitial production rates with increasing Ti content. This effect would prevent the formation of microvoids in the V–4.5Ti samples. The well-known scavenging effect of Ti on interstitial impurities can also contribute to inhibit the vacancy clustering in V–Ti.

4.3. V–Ti alloys. Second recovery stage

Now, we go on to discuss the positron lifetime increase found in the recovery curves preceding the second recovery stage, see Fig. 3. The same phenomenon is observed in cold-rolled samples of these V–Ti alloys [15]. It has been attributed to sinking of vacancies, released during recrystallization, into Ti-rich precipitates. The incorporation of these vacancies in the precipitate lattice results in non-stoichiometric precipitates with a very high affinity for positrons increasing the mean positron lifetime due to trapping at structural vacancies. This model cannot be claimed in the present case because the samples do not undergo recrystallization as they were irradiated after annealing at 1573 K.

There exists transmission electron microscopy (TEM) evidence for irradiation-induced precipitation of Ti-rich fine particles in V–Ti alloys. These precipitates have been identified as TiO_2 [4,25], TiO [26], Ti_2O [7] and Ti_3O [27]. The composition of these precipitates has not been well established because of the difficulty to perform reliable and accurate energy dispersive X-ray spectroscopy (EDS), or because electron diffraction analyses cannot identify the precipitates unambiguously [28]. Moreover, it appears that the precipitate composition depends on the irradiation conditions and post-irradiation thermal treatments. However, most of the authors identify the irradiation-induced precipitates as Ti oxides. TEM observations in neutron-irradiated V–4.5Ti show that precipitates do not appear for irradiation temperatures of 473 K but they do for irradiation temperatures $T \geqslant 623$ K [9]. That is, precipitates are formed when vacancies and interstitial impurities become mobile. Thus, precipitates in our samples would not be produced during irradiation but during recovery.

A careful inspection of the assessed Ti–O phase diagram shows that metastable phases such as $\beta Ti_{1-x}O$ and βTiO could be formed at $993 \leqslant T \leqslant 1093$ K and at $1093 \leqslant T \leqslant 1523$ K, respectively [29]. After cooling down, these metastable phases are decomposed into the low-temperature phases αTiO and βTi_2O_3 whose structures involve vacancy ordering [29]. The low values of the above temperature intervals, i.e., ~1000 K and ~1100 K, coincide with the annealing temperature for which

the positron lifetime increases in the recovery curves for V–4.5Ti and V–1Ti, respectively. This lifetime increase can be tentatively attributed to decomposition of these metastable phases formed during annealing. Because of the large lattice mismatch between the V matrix and these probable precipitated phases, a high concentration of dislocations and other vacancy-type defects is needed around the precipitates. Thus, the precipitate/matrix interfaces and the precipitate lattice would be biased sinks for vacancies. After cooling down, the low-temperature phases may be incongruently precipitated by decomposition of the metastable phase. For instance, the phase αTiO would not be completely stoichiometric, and its structural vacancies could be the positron traps responsible for the lifetime of 207 ps found after annealing above 1100 K in V–1Ti. Increasing the annealing temperature, the composition of the metastable phase can change giving a phase αTiO precipitated at RT each time more stoichiometric after the successive isochronal anneals. This accounts for the decreases of the intensity I_2 and mean lifetime $\langle\tau\rangle$ for V–1Ti after annealing above 1300 K.

Since Ti appears to decorate dislocations in V–4.5Ti, an enhancement of the Ti diffusion is expected in this alloy because of pipe diffusion along dislocations. Therefore, Ti migration and subsequent formation of the metastable phase may take place in V–4.5Ti at a lower temperature than in V–1Ti. The increase of the positron lifetime observed in the recovery curve for V–4.5Ti is lower because less irradiation-induced vacancies remain retained in these samples.

We rule out that the observed lifetime increase during recovery may be due to oxidation or contamination of the samples produced by the annealing treatments. We have not observed this effect in solution-annealed V–1Ti isochronally annealed up to above 1400 K [15]. Neither it is observed during the recovery of electron-irradiated V–Ga alloys [30].

5. Conclusions

Positron annihilation experiments indicate that a concentration of ~4.5 at.% Ti prevents the microvoid formation in V during neutron irradiation at 320 K. The swelling inhibition by Ti appears to be related to the solute Ti effect on the mutual recombination and clustering of vacancies and SIAs during irradiation. This effect is produced by vacancy trapping by solute Ti. The results reveal a large dislocation bias for vacancies and Ti preventing the vacancy coalescence into microvoids in V–4.5Ti, and the microvoid growth in V–1Ti, when vacancies become mobile. Microvoids formed in V–1Ti during irradiation anneal out above 683 K.

Although the positron lifetime recovery for the V–Ti alloys appears after annealing at ~600 K, the temperature dependence of the parameter S indicates that some microstructural defects acting as shallow positron traps anneal out of at temperatures below 533 K.

Precipitates of some metastable Ti oxides could be formed during post-irradiation annealing treatments above ~1000 K in V–Ti alloys. The decomposition of these precipitates into stable phases after cooling down can give rise to the appearance of vacancies retained into the precipitate lattice or at the matrix/precipitate interface. This would cause the positron lifetime increase observed preceding the second recovery stage.

Acknowledgements

This research was supported by the Dirección General de Enseñanza of Spain under contract No. PB95-0284. The irradiation was carried out in the High Flux Reactor of the Institute for Advanced Materials at Petten under contract No. 40.00024 with the European Atomic Energy Commission.

References

[1] R.E. Gold, D.L. Harrod, Int. Metals Rev. 25 (1980) 232.
[2] B.A. Loomis, D.L. Smith, J. Nucl. Mater. 191–194 (1992) 84.
[3] H. Matsui, K. Fukumoto, D.L. Smith, H.M. Chung, W. van Witzenburg, S.N. Votinov, J. Nucl. Mater. 233–237 (1996) 92.
[4] S. Ohnuki, D.S. Gelles, B.A. Loomis, F.A. Garner, H. Takahashi, J. Nucl. Mater. 179–181 (1991) 775.
[5] B.A. Loomis, A.B. Hull, D.L. Smith, J. Nucl. Mater. 179–181 (1991) 148.
[6] B.A. Loomis, D.L. Smith, F.A. Garner, J. Nucl. Mater. 179–181 (1991) 771.
[7] H.M. Chung, D.L. Smith, J. Nucl. Mater. 191–194 (1992) 942.
[8] H. Matsui, H. Nakajima, S. Yoshida, J. Nucl. Mater. 205 (1993) 452.
[9] H. Matsui, K. Kuji, M. Hasegawa, A. Kimura, J. Nucl. Mater. 212–215 (1994) 784.
[10] B.A. Loomis, L.J. Nowicki, D.L. Smith, J. Nucl. Mater. 212–215 (1994) 790.
[11] H.M. Chung, B.A. Loomis, D.L. Smith, J. Nucl. Mater. 212–215 (1994) 804.
[12] H. Nakajima, S. Yoshida, Y. Kohno, H. Matsui, J. Nucl. Mater. 191–194 (1992) 952.
[13] D.S. Gelles, J.F. Stubbins, J. Nucl. Mater. 212–215 (1994) 778.
[14] T. Leguey, R. Pareja, E.R. Hodgson, J. Nucl. Mater. 231 (1996) 191.
[15] T. Leguey, A. Muñoz, R. Pareja, J. Nucl. Mater. 275 (1999) 138.
[16] M.J. Puska, R.M. Nieminen, Rev. Mod. Phys. 66 (1994) 841.
[17] M. Eldrup, J. de Physique IV Colloque C1 5 (1995) 93.

[18] P. Kirkegaard, M. Eldrup, O.E. Mogensen, N.J. Pedersen, Comput. Phys. Commun. 23 (1981) 307.
[19] P. Hautojärvi, J. Heiniö, M. Manninen, Phil. Mag. 35 (1977) 973.
[20] T. McMullen, J. Phys. F 7 (1977) 3401.
[21] T. McMullen, J. Phys. F 8 (1979) 87.
[22] R.M. Nieminen, J. Laakkonen, P. Hautojärvi, A. Vehanen, Phys. Rev. B 19 (1979) 1397.
[23] L. Smedsjaer, M. Manninen, M. Fluss, J. Phys. F 10 (1980) 2237.
[24] T. Leguey, R. Pareja, J. Phys. 10 (1998) 2559.
[25] J.A. Sprague, F.A. Smidt, J.R. Reed, J. Nucl. Mater. 85–86 (1979) 739.
[26] Y. Higashiguchi, H. Kayano, S. Morozumi, J. Nucl. Mater. 133–134 (1985) 662.
[27] B.A. Loomis, B.J. Kestel, S.B. Gerber, Radiation-induced changes in the microstructure, in: F.A. Garner, N.H. Packan, A.S. Kumar (Eds.), ASTM STP 955. ASTM Philadelphia 1987, p. 730.
[28] D.S. Gelles, P.M. Rice, S.J. Kinkle, H.M. Chung, J. Nucl. Mater. 258–263 (1998) 1380.
[29] J.L. Murray, Phase Diagrams of Binary Titanium Alloys, ASM International, Metals Park, Ohio, 1987.
[30] T. Leguey, M.A. Monge, R. Pareja, E.R. Hodgson, this issue, p. 364.